Journal of GeoEngineering, Vol. 12, No. 1, pp. 21-34, March 2017
http://dx.doi.org/10.6310/jog.2017.12(1).3

ON THE SYSTEM STIFFNESS OF DEEP EXCAVATION IN SOFT CLAY

Hsii-Sheng Hsieh [1*], Yan-Hong Huang [2], Wei-Ting Hsu [3], and Louis Ge [4]

ABSTRACT

In urban area with soft clay deposit, it is required that the wall deformation of a deep excavation be limited to a very low value in order to minimize damages to adjacent buildings. Major factors that control the magnitude of wall deformation includes excavation depth, shear strength of soft clay, stiffness of bracing system, and flexural rigidity of retaining wall. The combined effect of bracing stiffness and flexural rigidity of retaining wall are often referred to as the system stiffness of an excavation. However, if low deformation is mandated in the design, the effects of auxiliary measures, such as soil improvement, buttress or cross walls, may also have to be incorporated as part of the system stiffness. In essence, the presence of auxiliary measures is equivalent to an increase of undrained shear strength of soft clay within the excavation zone, that in turn leads to an increase of passive resistance and a lower magnitude of wall deformation. The factor of safety against basal heave is also tied to the magnitude of undrained shear strength, therefore, reassessing the relationship between wall deformation and factor of safety against basal heave allows the authors to incorporate the effect of auxiliary measures in the framework of system stiffness. Four deep excavation cases in soft clay were presented in this paper, the effects of auxiliary measures were evaluated, and attempts were made to extend the system stiffness design curves into low deformation area. It is also noted that the 3-dimensional effect or preloading effect of soil mass within the excavation may overshadow the effect of system stiffness on wall deformation, provided that the factor of safety against basal heave is higher than 3.

Key words: Deep excavation, soft clay, system stiffness, wall deformation.

1. INTRODUCTION

The design of retaining system for deep excavations in soft clay has always been a challenge for geotechnical engineers. In early years, excessive movement of retaining wall and large settlement of adjacent ground were regarded as inevitable events, and the design engineers were just struggling to maintain the overall stability of excavations. One of the many lessons learned in these bizarre years is that the behavior of deep excavation is governed by the undrained shear strength (s_u) of soft clay, not by the total strength parameters c_u and ϕ_u acquired from conventional consolidated undrained triaxial tests (*CU* test). If c_u and ϕ_u were mistakenly used, it might lead to an unconservative excavation design that could in turn result in failure of the retaining system (Tsai 1994; Ou 2006). Figure 1 shows a classical failure case in early years when an over estimation on the passive resistance by using c_u and ϕ_u led to the eventual collapse of this excavation in soft clay.

As the designers learned from the failure cases and began to use s_u for excavation design in soft clay, excavation failure had not been reported for the past two decades. The attention on excavation design has shifted to another major issue, namely, the control of wall deformation. In addition to maintaining the overall stability of excavation, it is also imperative to limit the excavation induced retaining wall deformation to a very low value in urban area, especially when the project site is surrounded by fragile existing buildings. Experience has shown that buildings adjacent to an excavation are less prone to damage if excavation induced ground settlement is relatively small, and a low level of wall deformation is a prerequisite for a small ground settlement (Clough and O'Rourke 1990; Hsieh and Ou 1998).

Fig. 1 Excavation failure in soft clay, Taipei, 1988

Strengthening the retaining wall and bracing system appears to be a straightforward solution to minimize wall displacement, however, there are practical limits in implementing these schemes. For instances, the thickness of diaphragm wall must

Manuscript received July 5, 2016; revised September 22, 2016; accepted October 20, 2016.
[1] Senior Engineer (corresponding author), Trinity Foundation Engineering Consultants, Co., Ltd., 3rd floor, 28, Lane 102, Section 1, An-Ho Road, Taipei, Taiwan (e-mail: drhsieh@tfec.com.tw).
[2,3] Engineer, Trinity Foundation Engineering Consultants, Co., Ltd., 3rd floor, 28, Lane 102, Section 1, An-Ho Road, Taipei, Taiwan.
[4] Professor, Department of Civil Engineering, National Taiwan University, 1, Section 4, Roosevelt Road, Taipei, Taiwan.

comply with the capacity of excavation machines, and spacing of struts must not hinder the construction of basement structure, *etc*., These limitations forced the designers to adopt alternative or auxiliary measures to maintain the deformation at a low level, and these measures include the use of soil improvement, buttress walls and cross walls. In the past two decades, extensive use of soil improvement, buttress walls and cross walls had been found in routine deep excavation designs to minimize excavation induced wall displacement (Chien *et al*. 2004). In order to simplify the design process and fit into the framework of beam-on-elasto-plastic numerical model, the effects of these auxiliary measures are regarded as increases in undrained shear strength and horizontal modulus of subgrade reaction (K_h) of the soft clay (Hsieh and Lu 1999). Design experience accumulated over the years also shown that strengthening the bracing system alone has limited success on reducing the wall deformation, as a significant part of wall deformation is developed underneath the dredge line, and this part of wall deformation is beyond the reach of bracing system way above the dredge line. On the other hand, soil improvement, buttress walls and cross walls provide additional passive resistance below the dredge line, thus, they are more effective in refraining the lateral inward movement of retaining wall. It is not to say that the stiffness of bracing system is of no importance in minimizing the wall deformation, the essence is that auxiliary measures in conjunction with a stiff bracing system are required to maintain the wall deformation under a very low value specified in the design.

This paper considers that system stiffness of a deep excavation is the combined effect of three items, namely, the flexural rigidity of retaining wall, stiffness of bracing system, and contribution from the auxiliary measures. Early documents (Clough *et al*. 1989; Clough and O'Rourke 1990) defines system stiffness as a function of the flexural rigidity of retaining wall and stiffness of bracing system, neglecting the effect of auxiliary measures such as ground improvement, buttress walls and cross walls. Since current deep excavation designs focus much more on the control of deformation, auxiliary measures have to be incorporated as part of the design. It is the purpose of this paper to assess the contribution of soil improvement, buttress wall and cross wall on system stiffness, which would allow the designers to have a better understanding on the relationship between system stiffness and wall deformation when low excavation induced deformation is required as a major part of the design.

2. BACKGROUND

Clough *et al*. (1989) first presented the relationship between wall displacement, system stiffness and factor of safety against basal heave (F_b). As shown in Fig. 2, wall displacement is not only controlled by system stiffness, but also by F_b. A deep excavation with a low F_b value tends to yield a relatively large wall deformation even if the system stiffness is near its maximum value. For example, a relatively large system stiffness of 500 would yield a maximum wall displacement about 1% of the excavation depth if the F_b value is 1.0. However, if the F_b value increases to 2, the maximum wall displacement reduces to only 0.3% of the excavation depth, which is a 70% reduction under the same system stiffness. Practical use of Fig. 2 is that the designer can select a system stiffness that fulfill the requirements on wall displacement and ground movement, and design the retaining wall and bracing system accordingly.

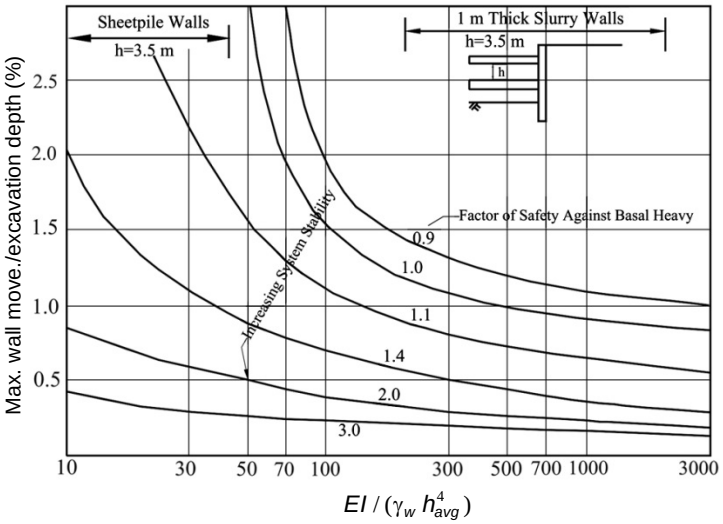

Fig. 2 Relationship between maximum wall movement and system stiffness (Redrawn from Clough *et al*. 1989)

The factor of safety against basal heave, F_b, is calculated based upon the equations defined by Terzaghi (1967). The *Y*-axis in Fig. 2 is the ratio between maximum wall displacement (δ_{hm}) and excavation depth (H_e), while the *X*-axis is the system stiffness (S) defined by Clough *et al*. (1989) as:

$$S = \frac{EI}{\gamma_w h_{avg}^4} \tag{1}$$

where EI is the flexural stiffness of retaining wall; γ_w is the unit weight of water; and h_{avg} is the average vertical spacing of bracing system.

Three parameters are included in Fig. 2, including normalized wall displacement, system stiffness and factor of safety against basal heave. The curves shown in Fig. 2 display roughly the relationship between normalized wall displacement, system stiffness and factor of safety against basal heave. Normalizing the wall displacement (δ_{hm}) with respect to excavation depth (H_e) has the implication that the magnitude of wall displacement is more or less proportional to the excavation depth. The system stiffness (S) as defined by Clough *et al*. (1989) is a dimensionless factor covering the flexural rigidity of retaining wall (EI) and average vertical spacing of bracing system (h_{avg}), implying that the behavior of retaining system is synonymous to a structural beam resting upon several supporting points. The factor of safety against basal heave (F_b) is a function of the excavation width (B) and undrained shear strength (s_u) of clay, that more or less covers the effects of site dimension and soil strength on the wall displacement.

Construction experience in Taiwan area shows that the ratio between maximum wall displacement and excavation depth is about 0.5% to 1.2% for excavations in soft clay, that falls in the lower half of Fig. 2. And most deep excavations in Taiwan urban area use stiff diaphragm wall together with horizontal struts with vertical spacing less than 3 m as the retaining system, that leads to a system stiffness generally higher than 200. In general, engineers in Taiwan use mostly the lower right corner of Fig. 2 as a guide for excavation design.

3. SCHEMES TO LIMIT WALL DISPLACEMENT

It is a well known fact that excavation in soft clay will experience excessive wall deformation. Large wall deformation can mostly be attributed to the low shear strength of soft clay, but other factors, such as the rigidity of retaining wall, stiffness of bracing system, amount of preload, installing sequence of struts, can also affect the magnitude of wall deformation. In the past, efforts had been made to reduce the wall deformation by either increasing the wall thickness, enhancing the strut stiffness, or adding more struts. Though effective to certain extent, these measures had their practical limits, and in many cases with stringent requirement on wall deformation, these measures simply fail to meet the design criterion by a wide margin. In other words, it is almost impossible to control the wall deformation under a specified low value for excavations in soft clay if strengthening retaining wall and bracing system are the only schemes available to the designers.

If a very small wall deformation is required to avoid damaging adjacent buildings, one of the most viable schemes would be to strengthen the soft soil on the passive side of the excavation. One often adopted approach in early years is to partially improve the ground within excavation either by jet grouting or soil mixing techniques (Hsieh *et al*. 1991; Woo 1992; Hsieh *et al*. 2003). The improvement ratio, which specifies the amount of improvement in percentage on the total volume of the improved soil mass, is one of the key design factors. In general, an improvement ratio higher than 12.5% is needed to have a marked effect on reducing wall deformation. A higher improvement ratio is even better in limiting wall displacement, but at the expense of skyrocketing construction cost. The soil improvement scheme also comes with other side effects, among which are the difficulties in quality control for a large number of improvement piles, and the risk of retaining wall being pushed significant outward by a poorly controlled jet grouting operation (Hsieh *et al*. 2002). In view of all the down-side experiences with soil improvement, current excavation designs are gradually shifting to an alternative scheme that uses buttress walls or cross walls to strengthen the overall stiffness of bracing system. In design practice, the effect of buttress walls or cross walls is modeled as a special type of soil improvement, and passive resistance of the excavation is increased as a result of their presence. Intuitively, the increment of passive resistance is proportional to the improvement ratio, or to the total amount of buttress walls or cross walls adopted in the design.

Contemporary deep excavation designs have a much more different facet than the designs 20 to 30 years ago. Several additional factors must also be considered in calculating the wall displacement, including preload of struts, horizontal spacing of struts, size of struts, effects of soil improvement, buttress walls, and cross walls. These factors have pronounced effects on limiting the magnitude of wall displacement, which is essential for excavations with stringent requirement on deformations. As for most of the excavations in Taiwan, the designers may have to keep the wall deformation below 0.2% of the excavation depth. And for some special cases with mass rapid transit tunnels or fragile buildings at close proximity, a wall deformation as low as 0.1% of the excavation depth may have to be enforced in the design. It is apparent that this requirement on a very low deformation has reached the limits of design curves shown in Fig. 2, and there is an urgent need to extend these curves further into the very low deformation region.

4. EFFECTS OF AUXILIARY MEASURES ON WALL DEFORMATION

Soil improvement, buttress walls and cross walls are generally considered as auxiliary measures in a deep excavation design to minimize excavation induced wall deformation. Approach is developed in this section to incorporate the effects of soil improvement, buttress walls and cross walls into the framework of system stiffness. As a construction practice, soil improvement piles, buttress walls or cross walls situate beneath the dredge line of each excavation stage. It is hypothesized that the contributions of these auxiliary measures are equivalent to an increase in undrained shear strength for soft clay underneath the dredge line, leading to an increase in the factor of safety against basal heave and a reduction in the wall deformation. In short, quantifying the effects of auxiliary measures via an increase in undrained shear strength would allow the designer to incorporate the auxiliary measures within a generalized framework of system stiffness.

4.1 Effect of Ground Improvement

The effect of ground improvement is equivalent to an increase in undrained shear strength of the improved soft clay. In order to control the improvement cost within an acceptable limit, ground is only partially improved in most cases. Discrete improvement piles with diameter ranging from 0.6 to 1 m are constructed with a typical spacing of 2 to 2.5 m. The improvement ratio (I_r), which is a key design parameter, is defined as the total cross sectional area of the improvement piles divided by the area of the improved site. An weighted average approach is adopted to calculate the equivalent strength of the improved ground (Wu 1989). This approach was successfully applied in numerous design cases for the last two decades, and it assumes the following form:

(a) Sandy soil:

$$c_m = (1 - I_r) \times c + \alpha \times I_r \times q_u / 2 \tag{2}$$

$$\phi_m = \phi \tag{3}$$

where c_m is the equivalent cohesion of the improved sandy ground; c is the cohesion of the before-improvement sandy ground; α is an empirical correction factor, which is generally taken as 2; q_u is the unconfined compressive strength of the improvement piles; ϕ_m is the equivalent friction angle of the improved sandy ground; and ϕ is the friction angle of the before-improvement sandy ground. As indicated by Eqs. (2) and (3), it is apparent that the friction angle of sandy soil is not affected by the improvement at all, while an equivalent cohesion is achieved as a result of improvement.

(b) Clayey soil:

$$s_{um} = (1 + I_r) \times s_u + \alpha \times I_r \times q_u / 2 \tag{4}$$

where s_{um} is the equivalent undrained shear strength of the improved ground and the empirical correction factor α is also taken as 2 for clayey soil. For a typical improvement ratio of 12.5% and a design q_u of 100 kPa, the equivalent undrained shear strength of the improved ground could reach 50 kPa for soft clay with an original s_u of 20 kPa according to Eq. (4).

4.2 Effect of Buttress Wall and Cross Wall

Most of the routine excavation designs were conducted by using a one-dimensional numerical program which considers the behavior of retaining wall as a beam resting upon an elasto-plastic foundation. Clearly, this type of one-dimensional numerical tool is not capable of fully modeling the 3-dimensional behavior of deep excavations that use buttress wall and cross wall as auxiliary measures. Though not perfect from a theoretical point of view, a simplified approach that transforms the effects of buttress wall or cross wall into an increase in shear strength parameters had been developed (Hsieh and Lu 1999), which allows the designers to incorporate the complex effects of buttress wall or cross wall in a routine 1-dimensional excavation analysis. Equations representing the effects of buttress wall and cross wall are given below, while details on the derivation of these equations can be found in reference (Hsieh and Lu 1999).

Equivalent Soil Strength Parameters

(a) Sandy soil:

$$K_p^* = K_p \times (1 + \tan\phi \times 2 \times L \times N_B / B) \tag{5}$$

where K_p^* is the equivalent passive earth pressure coefficient; K_p is the passive earth pressure coefficient; L is the length of buttress wall or cross wall; N_B is the number of buttress wall or cross wall for a site with width B; and B is the width of the excavation.

(b) Clayey soil:

$$s_u^* = s_u \times (1 + L \times N_B / B) \tag{6}$$

where s_u^* is the equivalent undrained shear strength with the installation of buttress wall or cross wall. It is clearly indicated in Eqs. (5) and (6) that the equivalent shear strength parameters are closely related to the number and length of buttress wall or cross wall.

Equivalent Horizontal Modulus of Subgrade Reaction

(a) Sandy soil:

$$K_h^* = K_h + 0.4N \times L \times N_B / B \tag{7}$$

where K_h^* is the equivalent horizontal modulus of subgrade reaction with the installation of buttress wall or cross wall; K_h is the horizontal modulus of subgrade reaction of the original ground; and N is the blow count of standard penetration test for sandy soil. Please note that the factor 0.4 in Eq. (7) is not dimensionless, it has the same unit as K_h.

(b) Clayey soil:

$$K_h^* = K_h \times (1 + L \times N_B / B) \tag{8}$$

4.3 Effect of Site Dimension

Experience has shown that for a relatively small excavation site in soft clay, the observed wall deformation is much smaller than the result predicted by a 1-dimensional or 2-dimensional numerical analysis. The over prediction on wall deformation can be attributed to the fact that 3-dimensional or corner effect of a small site is often neglected in the excavation design as pointed out by Ou *et al*. (1996) and Finno *et al*. (2007). Ou *et al*. (1996) provided a design chart that gives a PSR (Plane strain ratio) value based upon the site dimension. The PSR value allows the engineer to roughly calculate the wall displacement under 3-dimensional condition. Finno *et al*. (2007) summarized their 3-dimensional numerical results and presented an equation to calculate the deformation ratio between 3-dimensional and plane strain conditions.

For a typical small site with perimeter diaphragm wall, a simple approach to model the 3-dimensional effect is to consider the perimeter diaphragm wall perpendicular to the main diaphragm walls as buttress walls or cross walls. In other words, 3-dimensional effect can also be modeled as an increase in shear strength of the soft ground (Hsieh *et al*. 2015).

5. EXCAVATION CASE HISTORIES

This section presents four deep excavation cases to delineate the effects of soil improvement, buttress wall as well as cross wall on the system stiffness and wall displacement. Displacements of diaphragm wall for each case were evaluated via the use of a computer code TORSA (Taiwan Originated Retaining Structure Analysis) published by Sino-Geotechnics Research and Development Foundation (2016), which is a beam-on-elasto-plastic-foundation program assuming the excavation is under a plane strain condition. The required input parameters of TORSA include unit weight, shear strength parameters and K_h of soils, flexural rigidity of retaining wall, axial stiffness and preload of bracing system, excavation sequence, ground water level, length and number of buttress/cross wall, ratio and strength of ground improvement, *etc*. Detailed description on the TORSA input parameters can be found in the TORSA user's manual (TORSA 2016).

These four sites situated within Taipei basin, all with thick soft clay layer that dominates the behavior of each excavation. The soft clay layer has typical standard penetration test (SPT) N values ranging from 2 to 4, the natural water content is about 35% to 50%. Detailed descriptions on the physical and engineering properties of the soft clay layer can be found in reference (Woo and Moh 1990).

5.1 Case I

Case I is a 17-story office building with 4 levels of basement, the excavation depth of basement is 17.1 m. The project site is about 40 m in length and 38 m in width. Excavation of the basement uses a diaphragm wall 0.8 m in thickness and 34 m in depth together with 5-level of *H*-steel bracings as the retaining system. The typical horizontal spacing of *H*-steel bracing is 6 m, and each level of bracing is preloaded to 50% of its allowable axial capacity. As shown in Fig. 3, four cross walls 0.8 m in thickness span the project site. Depth of the cross walls extends from GL.–16 m to GL.–34 m. Also shown in Fig. 3 are six inclinometer casings (SID-1 to SID-6) installed in the perimeter diaphragm wall to monitor the wall deformation for each stage of excavation. Simplified soil profile and soil parameters are presented in Table 1. Ground water level is at GL.–2 m.

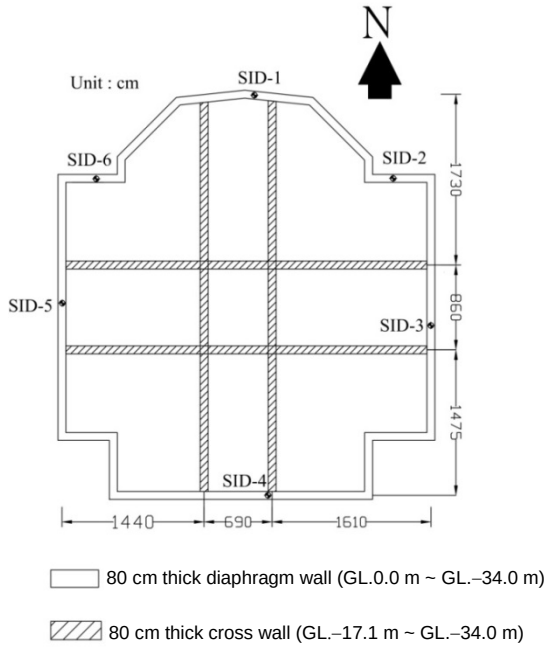

Fig. 3 Layout of diaphragm wall and cross walls for Case I

Table 1 Simplified soil profile and parameters of Case I

Layer	Depth (m)	Type	SPT-N	γ_t (kN/m^3)	c' (kPa)	ϕ' (deg)	s_u (kPa)
1	0 ~ 3.5	CL	5	18.7	–	–	54.0
2	3.5 ~ 9.3	SM	8	20.0	0	31	–
3	9.3 ~ 24.2	CL	3	18.6	0	27	32.4
4	24.2 ~ 30.4	CL	6	18.6	0	30	58.9
5	30.4 ~ 32.8	ML/SM	9	18.7	0	31	–
6	32.8 ~ 45.4	CL	10	18.3	0	31	98.1
7	45.4 ~ 48.4	CH	15	18.2	–	–	107.9
8	48.4 ~ 56.1	CL	19	19.1	–	–	135.4
9	56.1 ~ 59.9	GM	> 100	21.6	–	–	–

The excavation sequence of Case I is shown in Table 2, including the sizes and preloads of horizontal struts. For each side, the perimeter diaphragm walls perpendicular to this specific side are also considered as cross walls, therefore there are in total 4 cross walls acting on each side of perimeter diaphragm wall. Wall displacements on each side of the construction site were evaluated by TORSA and compared with field results as shown in Fig. 4. It is found that the TORSA predictions are much higher than the field observations. In general, the observed maximum wall displacements are less than 10 mm, while TORSA predictions are in the vicinity of 25 mm. The discrepancies can be attributed to the TORSA's limited capability in modeling the 3-dimensional behavior of a small site, especially for a small site with very pronounced 3-dimensional effect.

It is obvious that installing two cross walls in each direction had significant impact on the wall deformation. TORSA predictions showed that the maximum wall displacement is less than 0.15% of the excavation depth, while field measurements showed even less, none of the inclinometer casings deformed more than 0.05% of the excavation depth. For a system stiffness ratio $EI / \gamma_w h_{avg}^4$ of around 1000, the TORSA predictions and field measurements are both underneath the design curves proposed by Clough *et al*. (1989), suggesting that design curves may not be applicable for cases with very low wall deformations. One approach to realign Clough's design curves in this case is to incorporate the effect of cross walls in the calculation of factor of safety against basal heave (F_b), and re-establish the relationship between wall displacement, system stiffness and F_b in the low displacement zone.

5.2 Case II

Case II is located in Hsin-yi district of Taipei city, which is a relatively large site with a footprint of about 12000 m^2. Length and width of the site are about 167 m and 68 m, respectively. The excavation depth of the 4-level basement is 20.05 m, using diaphragm wall 1m in thickness and 41 m in depth as the retaining wall. The basement excavation was carried out by a conventional top-down scheme using floor slabs as lateral supports. As shown in Fig. 5, 3 cross walls and a total of 21 buttress walls are adopted as the auxiliary measures in an effort to limit the excavation induced wall displacement. Length of buttress wall is 8.5 m, 10 m or 12 m, pending on location of the buttress wall. Subsurface condition of this site consists mainly of soft to medium stiff silty clay as shown in Table 3. Ground water level was at about GL.–1 m.

Table 2 Bottom-up excavation sequence of Case I

Stage	Activity	Remarks
1	Excavate to GL.–1.7 m	First exc. stage
2	Install strut at GL.–1.0 m	H300 × 300 × 10 × 15 mm Preload: 490 kN/ea
3	Excavate to GL.–4.8 m	Second exc. stage
4	Install strut at GL.–4.1 m	H400 × 400 × 13 × 21 mm Preload: 980 kN/ea
5	Excavate to GL.–8.0 m	Third exc. stage
6	Install strut at GL.–7.3 m	2H400 × 408 × 21 × 21 mm Preload: 980 kN/ea
7	Excavate to GL.–11.2 m	Fourth exc. stage
8	Install strut at GL.–10.5 m	2H400 × 408 × 21 × 21 mm Preload: 980 kN/ea
9	Excavate to GL.–14.4 m	Fifth exc. stage
10	Install strut at GL.–13.7 m	2H400 × 408 × 21 × 21 mm Preload: 980 kN/ea
11	Excavate to GL.–17.1 m	Final exc. stage

kN/ea : axial load/each strut

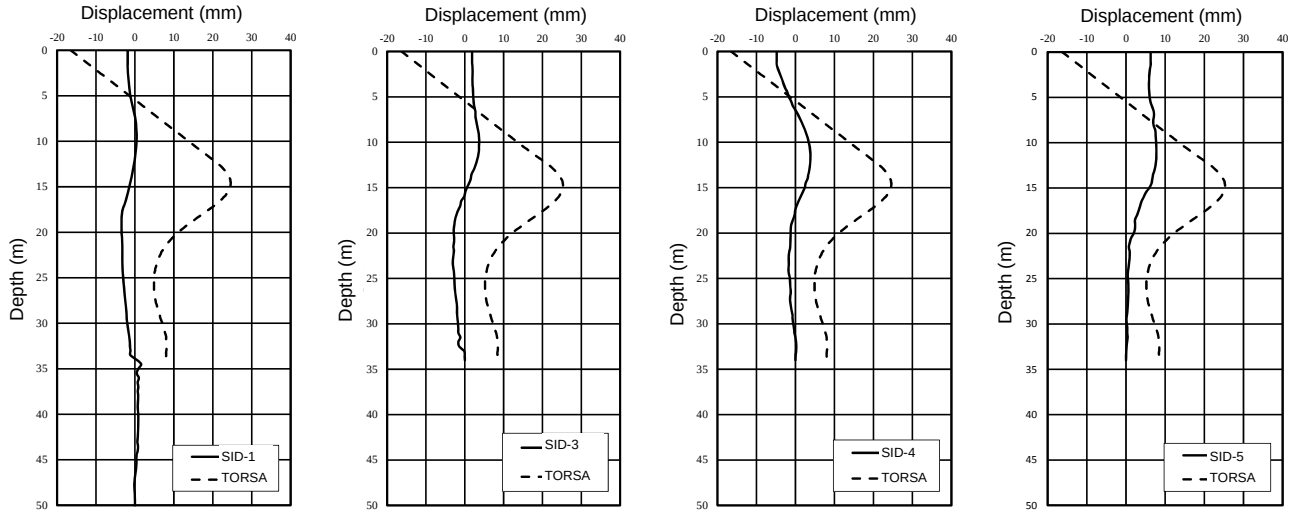

Fig. 4 Comparison of wall displacements for Case I

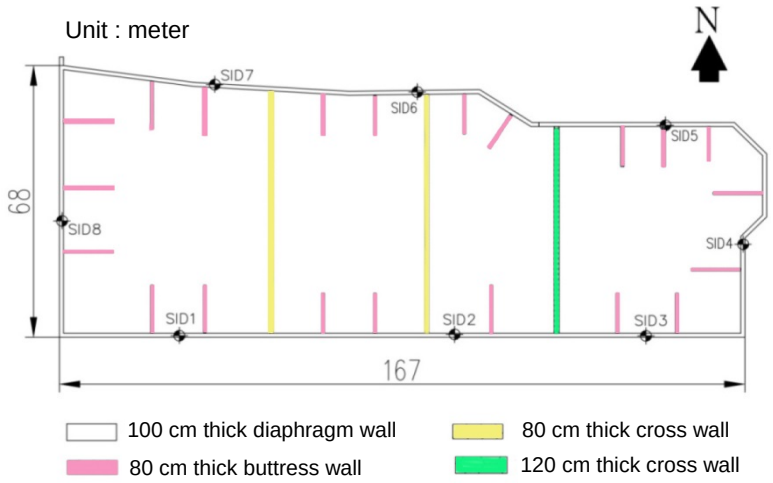

Fig. 5 Layout of diaphragm wall, buttress walls and cross walls for Case II

Table 3 Simplified soil profile and parameters of Case II

Layer	Depth (m)	Type	SPT-N	γ_t (kN/m^3)	c' (kPa)	ϕ' (deg)	s_u (kPa)
1	0.0 ~ 1.0	Fill	–	18.1	0	28	–
2	1.0 ~ 2.4	CL	1.5 ~ 5 (3)*	17.6	9.8	27	29.4
3	2.4 ~ 14.1	CL	1 ~ 6 (2)*	17.9	1.0	27	24.5 ~ 29.4
	14.1 ~ 21.6		2 ~ 5 (3.5)*	18.0	1.0	28	29.4 ~ 49.1
	21.6 ~ 32.3		4 ~ 19 (7)*	18.3	1.0	30	49.1 ~ 68.7
4	32.3 ~ 33.9	SM/ML	9 ~ 32 (16)*	18.4	0	31	–
5	33.9 ~ 39.0	CL	6 ~ 24 (11)*	18.7	9.8	30	88.3
6	39.0 ~ 41.3	SM/ML	9 ~ 45 (25)*	19.1	0	32	–
7	41.3 ~ 47.9	CL/SM	10 ~ 47 (20)*	19.5	9.8	30	117.7
8	47.9 ~ 51.3	SM	27 ~ 48 (39)*	19.8	0	34	–
9	51.3 ~ 54.3	GW1	> 50	20.6	0	40	–

Note: numbers in parenthesis are average F_b and $\delta_{\text{in-situ}} / H_e$ for each case

Excavation sequence of Case II is listed in Table 4, while the comparison of the TORSA predictions and field measurements on wall displacements are shown in Fig. 6. Since this is a relatively large site, 3-dimensional effect is less significant in this case, resulting in a better agreement between TORSA predictions and observed wall displacements. Locations of inclinometer casings SID-2 and SID-6 are close to one of the cross walls, therefore corner effects are evident and less wall deformations were observed at these two locations. The inclinometer casing SID-8 shows significant wall movement in excess of 120 mm in the mid-section of west side, which is much higher than other readings shown in Fig. 6. Possible explanation for this large wall deformation is that west side is the driveway to basement parking, openings on the floor slab significantly reduce the stiffness of lateral supports on west side, leading to a wall deformation much higher than expected.

Table 4 Top-down excavation sequence of Case II

Stage	Activity	Remarks
1	Excavate to GL.–2.5 m	First exc. stage
2	Cast 1FL at GL.0 m	Slab thickness: 0.2 m
3	Excavate to GL.–7.65 m	Second exc. stage
4	Cast B1FL at GL.–5.65 m	Slab thickness: 0.2 m
5	Excavate to GL.–12.65 m	Third exc. stage
6	Cast B2FL at GL.–10.65 m	Slab thickness: 0.45 m
7	Excavate to GL.–16.05 m	Fourth exc. stage
8	Cast B3FL at GL.–14.05 m	Slab thickness: 0.45 m
9	Excavate to GL.–17.45 m	Fifth exc. stage
10	Install strut at GL.–16.65 m	2H400 × 400 × 13 × 21 mm Preload: 980 kN/ea
11	Excavate to GL.–20.05 m	Final exc. stage

kN/ea : axial load/each strut

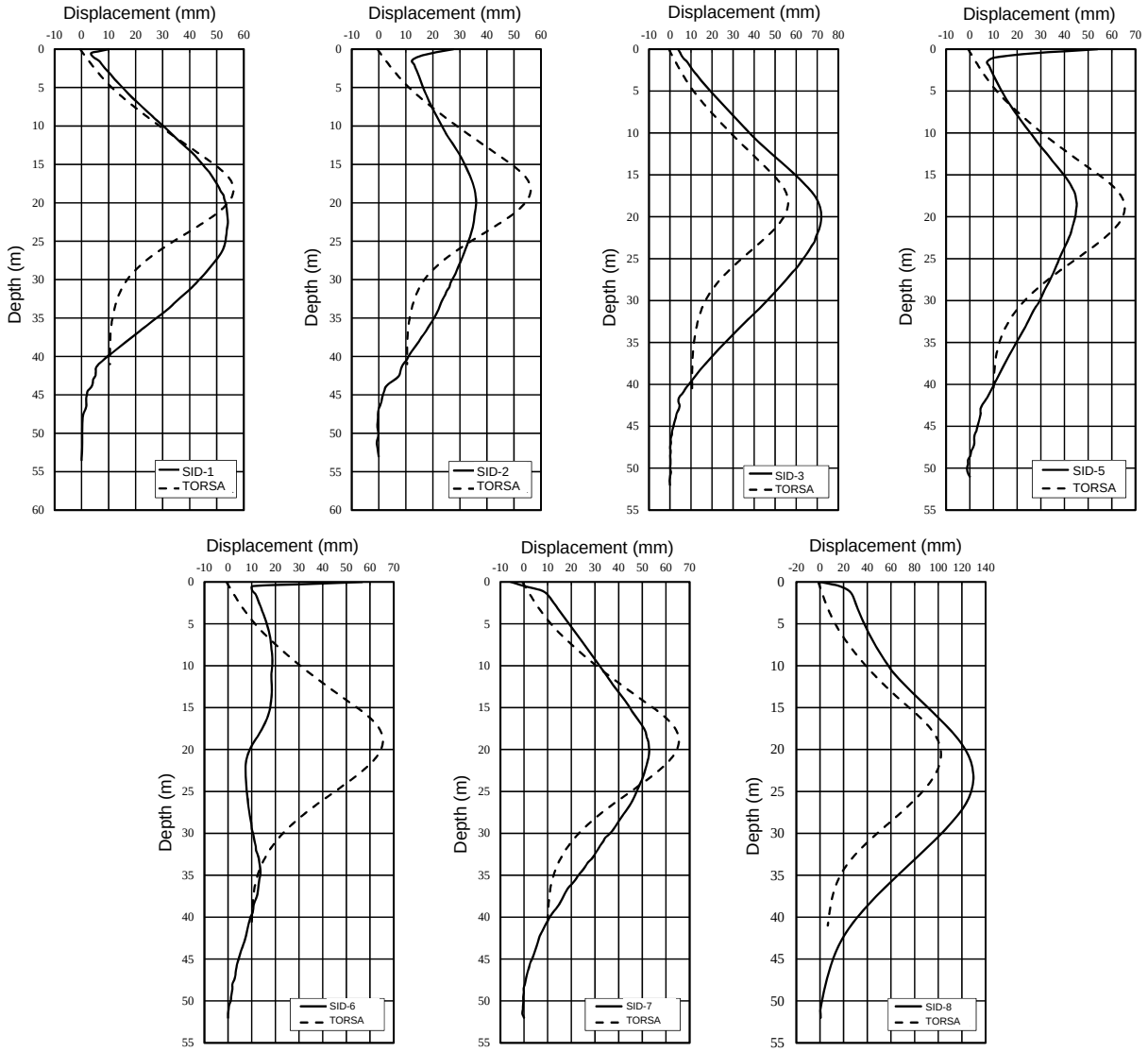

Fig. 6 Comparison of wall displacements for Case II

Case II basement was excavated predominately in soft clay, the deformation of diaphragm wall could have been excessive if auxiliary measures such as cross walls and buttress walls had not been implemented. The effect of cross walls and buttress walls can also be transformed into an increase in undrained shear strength, leading to an increase in factor of safety against basal heave and a reduction in wall deformation. Even with the extensive use of cross walls and buttress walls, Case II still behaved as a large site governed by plane strain condition, which is evident by the close agreements between TORSA predictions and field curves.

5.3 Case III

Case III is also located in Hsin-yi district of Taipei city (Kuo *et al*. 2014), which is a very small site with a footprint of about 550 m^2. Length and width of the site are about 26 m and 21 m, respectively. The project site was originally occupied by a high-rise building with 3-level of basement, and the owner decided to demolish the old building in favor of a new 14-story building with 4-level of basement. The original 3-level basement was excavated to GL.–14.2 m, using a 0.7 m thick diaphragm wall 25 m in depth as the retaining wall. The excavation depth of the new 4-level basement is 21.5 m, requiring the use of a 34 m deep diaphragm wall as part of the retaining system. As it turned out, the original 3-level basement was a humongous obstacle to the construction of the new diaphragm wall and new basement, and the contractor was forced to use the original diaphragm wall, which is of inadequate depth and stiffness, as the retaining wall to excavate the new basement. To avoid excavation failure as a result of insufficient stability, auxiliary measure in the form of soil improvement was adopted to strengthen the overall stiffness of retaining system. Jet grouted piles were installed within the project site with a layout shown in Fig. 7. The improvement ratio is 64%, which is much higher than the 12.5% used in typical projects. The jet grouted piles varied in diameter and length as shown in Fig. 7, but all with the same unconfined compressive strength of 100 MPa. Site geometry and locations of inclinometer casings are also presented in Fig. 7. Subsurface condition of this site consists of six main layers with thickness and parameters shown in Table 5. Ground water level was at about GL.–3 m. Excavation of basement was conducted by a mixed scheme using 6 levels of horizontal bracings and one level of basement floor as the lateral supports. Excavation sequence of Case III is listed in Table 6 for reference.

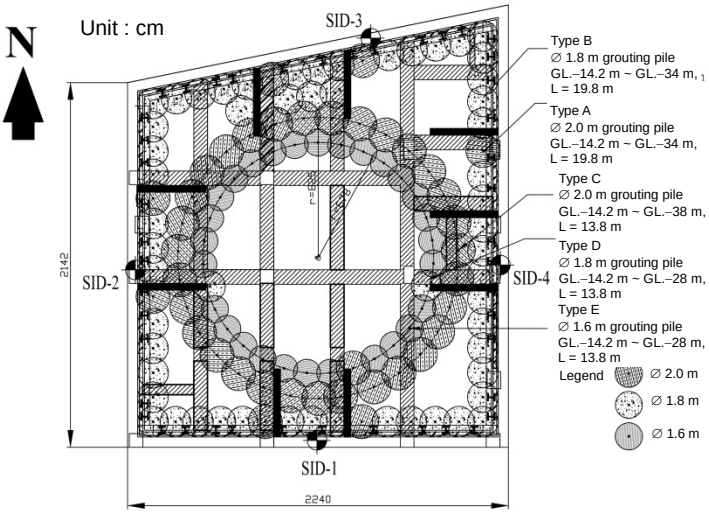

Fig. 7 Layout of diaphragm wall and jet grouted piles for Case III

Table 5 Simplified soil parameters of Case III

Layer	Depth (m)	Type	SPT-N	γ_t (kN/m^3)	c' (kPa)	ϕ' (deg)	s_u (kPa)
1	0 ~ 4.7	Fill/CL	2 ~ 6 (5)*	18.4	0	–	19.6
2	4.7 ~ 16.8	GM/SM	6 ~ > 50 (28)*	20.0	0	33	–
3	16.8 ~ 27.4	CL	4 ~ 18 (9)*	17.9	0	–	39.2 ~ 63.8
4	27.4 ~ 32.8	ML/SM	10 ~ 34 (18)*	19.2	0	31	–
5	32.8 ~ 44.6	GM/SM/CL	10 ~ > 50 (12)*	18.6	0	29	–

Note: numbers in parenthesis are average F_b and $\delta_{\text{in-situ}} / H_e$ for each case

Table 6 Mixed bottom-up/top-down excavation sequence of Case III

Stage	Activity	Remarks
1	Excavate to GL.–3.0 m	First exc. stage
2	Install strut at GL.–2.0 m	H350 × 350 × 12 × 19 mm Preload: 490 kN/ea
3	Excavate to GL.–6.3 m	Second exc. stage
4	Install strut at GL.–5.3 m	H400 × 400 × 13 × 21 mm Preload: 980 kN/ea
5	Excavate to GL.–9.65 m	Third exc. stage
6	Install strut at GL.–8.653 m	H400 × 400 × 13 × 21 mm Preload: 980 kN/ea
7	Excavate to GL.–12.1 m	Fourth exc. stage
8	Install strut at GL.–11.1 m	2H400 × 408 × 21 × 21 mm Preload: 980 kN/ea
9	Excavate to GL.–16.0 m	Fifth exc. stage
10	Cast slab at GL.–14.6 m	B3 floor slab
11	Excavate to GL.–18 m	Sixth exc. stage
12	Install strut at GL.–17.0 m	2H400 × 408 × 21 × 21 mm Preload: 980 kN/ea
13	Excavate to GL.–20.0 m	Seventh exc. stage
14	Install strut at GL.–19.0 m	2H400 × 408 × 21 × 21 mm Preload: 980 kN/ea
15	Excavate to GL.–21.5 m	Final exc. stage

kN/ea : axial load/each strut

Site dimension of Case III is even smaller than that of Case I. The ratio of site width to excavation depth is close to 1.2, which is expected to exhibit pronounced 3-dimensional effect as suggested by Finno *et al*. (2007). And as a result of the pronounced 3-dimensional effect, the observed wall displacements are likely to be much smaller than TORSA predictions. As shown in Fig. 8, the maximum wall displacement predicted by TORSA is about 35 mm, while the observed wall displacement is in the vicinity of 15 mm (SID-4), which is a clear indication that the overall system stiffness of this small site is under estimated by TORSA. Also noted in Fig. 8, inclinometer casing SID-1 shows a peculiar deformation pattern as it is pushed outward by an amount of 5 mm near the final excavation depth, which is probably a collateral effect induced by the operation of jet grouting (Hsieh *et al*. 2002).

The system stiffness of the retaining system for Case III is markedly affected by the implementation of soil improvement. The effect of soil improvement is equivalent to an increase in undrained shear strength, which in turn leads to an increase in factor of safety against basal heave and a reduction in wall displacement. The maximum wall displacement in this case is about 0.07% of the excavation depth, which situates in a position significantly lower than design curves shown in Fig. 2. In addition to the effect of soil improvement, it appears that other factors, including the 3-dimensional effect of a small site and preloading effect by the application of jet grouting (Hsieh *et al*. 2003), may also contribute in limiting the wall displacement to such a small magnitude.

5.4 Case IV

Case IV is the UP building which is a 35-story office building with a 7-level basement (Ou et al. 2006). The project site is 120 m in length and 63 m in width, and the excavation depth of basement is 32.5 m. Diaphragm wall 1.5 m in thickness and 55 m in depth is used as the retaining wall, and the basement was excavated by a top-down scheme using basement slabs as excavation supports. In the period of basement construction, there were no buildings around the project site, but there were concerns about the lateral displacements of diaphragm wall as the excavation depth exceeded a mentally tolerable limit of 30 m. To minimize the diaphragm wall displacements, cross walls and buttress walls were installed within the construction site with a plan layout shown in Fig. 9. The depths of cross walls and buttress walls are 55 m and 45 m, respectively. The readings of inclinometer casings at mid-section of each side were used to study the effect of cross walls and buttress walls as those inclinometer casings were less affected by corner effects. As shown in Fig. 9, SID-4, SID-2, SID-9 and SID-7 are the inclinometer casings located at mid-section of east, south, west and north sides of the project site, respectively. Subsurface of the project site consists mainly of soft to medium stiff clay, the thickness and parameters of each layer are presented in Table 7. As indicated by the readings of observation wells, the ground water level was at 3 m below surface.

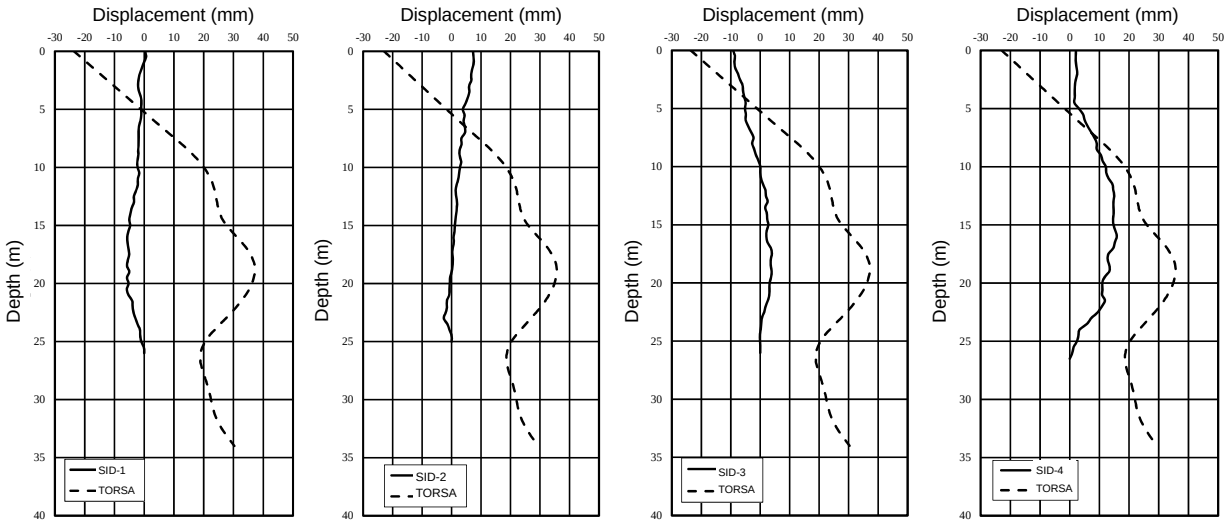

Fig. 8 Comparison of wall displacements for Case III

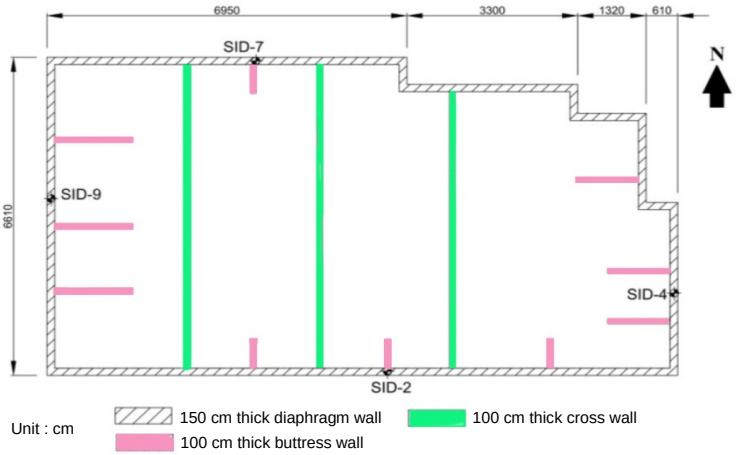

Fig. 9 Layout of diaphragm wall, buttress walls and cross walls for Case IV

The excavation sequence is listed in Table 8. Figure 10 is the comparison between measured wall displacements and the TORSA simulation results. Since the project site is relatively large in dimension, wall displacements were less affected by 3-dimensional or corner effect. As a result, discrepancies between field data and predictions were found to be less significant, the maximum wall displacements were all less than 100 mm.

In general, Cases II and IV are similar in excavation behavior. Both cases are large sites using top-down excavation scheme, and the predicted wall displacements are found to be close to the design curves presented in Fig. 2. This finding is perhaps an indication that the current approach to simulate the effects of cross walls and buttress walls as an increase in undrained shear strength can correctly predict the variation in system stiffness when cross walls and buttress walls are incorporated in the excavation design for large sites.

Table 7 Simplified soil parameters of Case IV

Layer	Depth (m)	Type	SPT-N	γ_t (kN/m^3)	c' (kPa)	ϕ' (deg)	s_u (kPa)
1	0.0 ~ 3.0	Fill	3 ~ > 50	18.2	0	30	–
2	3.0 ~ 32.6	CL	1 ~ 18	18.1	0	–	19.6 ~ 78.5
3	32.6 ~ 51.0	CL	7 ~ 37	18.7	0	–	78.5 ~ 127.5
4	51.0 ~ 66.7	SM/GW	> 50	19.6	0	35 ~ 38	–
5	> 66.7	Rock	> 50	–	–	–	490.5

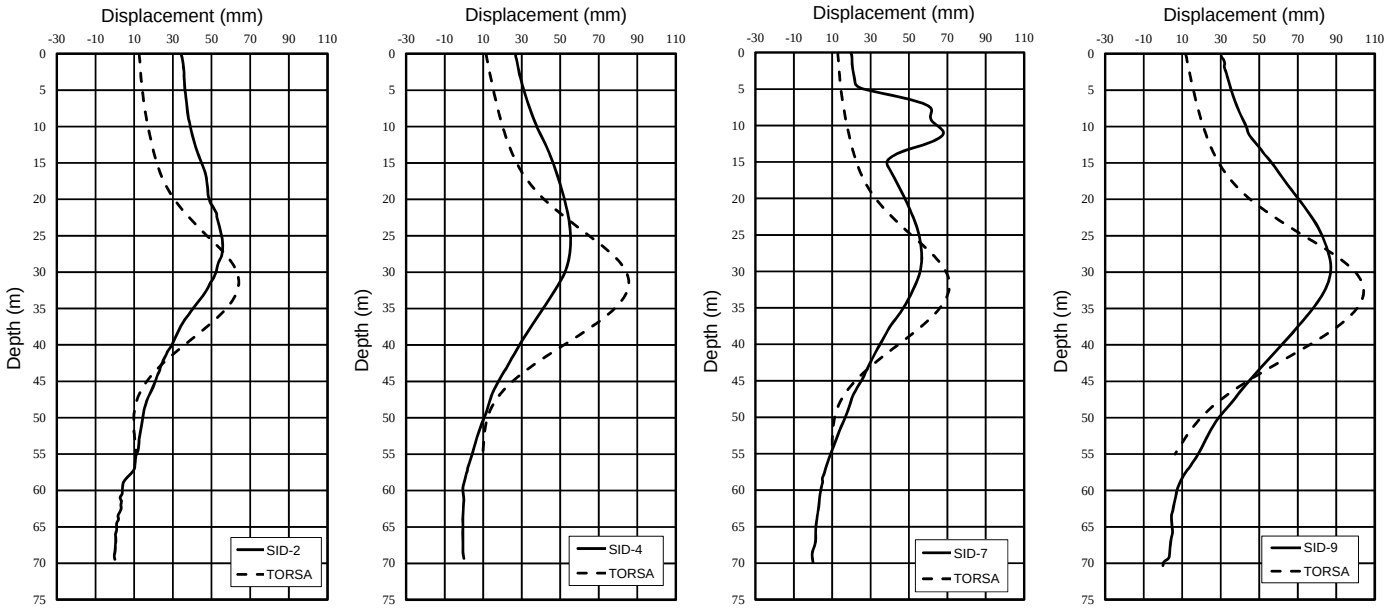

Fig. 10 Comparison of wall displacements for Case IV

Table 8 Top-down excavation sequence of Case IV

Stage	Activity	Remarks
1	Excavate to GL.–3.5 m	First exc. stage
2	Cast 1FL at GL.0 m	Slab thickness: 0.25 m
3	Excavate to GL.–6.05 m	Second exc. stage
4	Cast B1FL at GL.–4.4 m	Slab thickness: 0.2 m
5	Excavate to GL.–10.45 m	Third exc. stage
6	Cast B2FL at GL.–9.0 m	Slab thickness: 0.61 m
7	Excavate to GL.–148 m	Fourth exc. stage
8	Cast B3FL at GL.–13.4 m	Slab thickness: 0.61 m
9	Excavate to GL.–18.15 m	Fifth exc. stage
10	Cast B4FL at GL.–16.8 m	Slab thickness: 0.61 m
11	Excavate to GL.–21.5 m	Sixth exc. stage
12	Cast B5FL at GL.–20.5 m	Slab thickness: 0.61 m
13	Excavate to GL.–26.05 m	Seventh exc. stage
14	Cast B5FL at GL.–24.8 m	Slab thickness: 0.61 m
15	Excavate to GL.–29.4 m	Eighth exc. stage
16	Install strut at GL.–29.4 m	2H428 × 407 × 201 × 35 mm Preload: 1176 kN/ea
17	Excavate to GL.–32.5 m	Final exc. stage

6. RELATIONSHIP BETWEEN SYSTEM STIFFNESS AND WALL DISPLACEMENT

Numerical and monitoring results of the four case histories presented above were summarized in this section to delineate the effects of auxiliary measures on system stiffness. First, program TORSA was used to calculate the baseline wall displacements of these four cases without the application of soil improvement, buttress wall or cross wall. The baseline wall displacements were then compared with the design curves proposed by Clough et al. (1989), and the results are shown in Table 9. If not assisted by auxiliary measures, excavations in soft clay are to have maximum wall displacements ($\delta_{baseline}$) 0.7% to 1.3% of the excavation depth as indicated in Table 9. On the other hand, Clough's design curves showed that the maximum wall displacements (δ_{Clough}) are about 0.2% to 0.3% the excavation depth, which are much lower than the baseline results. Possible explanation for the discrepancy is that outcomes of TORSA analyses are sensitive to the undrained shear strength of soft clay, especially for $s_u / \sigma'_v < 0.3$, that low s_u / σ'_v values generally yield high wall displacements. Another possible reason is that the factors of safety against basal heave in these four cases cannot be calculated via a straightforward manner, the undrained shear strength below or above dredge line varies with depth, requiring an engineering judgment to select appropriate values for the calculation of F_b, and the determination of δ_{Clough} may be affected as a result.

The comparison between $\delta_{baseline}$ and δ_{design} of the four cases is presented in Table 10, in which $\delta_{baseline}$ and δ_{design} are maximum wall

Table 9 Comparison between baseline displacements and Clough's design values

Case	SID	$F_{b\_baseline}$	$\delta_{baseline}$ (cm)	$EI / \gamma_w h_{avg}^4$	$\delta_{baseline} / H_e$ (%)	δ_{Clough} / H_e (%)
I	1	1.63	15.26	986	0.89	0.32
	3	1.64	15.25	986	0.89	0.32
	4	1.63	15.26	986	0.89	0.32
	5	1.64	15.25	986	0.89	0.32
II	1	1.97	22.54	540	1.12	0.26
	2	1.97	22.54	540	1.12	0.26
	3	1.97	22.54	540	1.12	0.26
	5	1.97	22.89	540	1.14	0.26
	6	1.97	22.89	540	1.14	0.26
	7	1.97	22.89	540	1.14	0.26
	8	1.97	26.1	540	1.30	0.26
III	1	2.4	15.19	829	0.71	0.21
	2	2.4	14.75	829	0.69	0.21
	3	2.4	15.19	829	0.71	0.21
	4	2.4	14.75	829	0.69	0.21
IV	2	1.6	28.01	2122	0.86	0.29
	4	1.6	31.85	2122	0.98	0.29
	7	1.6	27.8	2122	0.86	0.29
	9	1.6	31.85	2122	0.98	0.29

Table 10 Comparison between baseline and design displacements

Case	SID	$F_{b\_baseline}$	F_{b_design}	$\delta_{baseline}$ (cm)	δ_{design} (cm)	$F_{b\_design} / F_{b\_baseline}$	$\delta_{design} / \delta_{baseline}$ (%)
I	1	1.63	3.2	15.26	2.47	1.96	16
	3	1.64	3.1	15.25	2.54	1.89	17
	4	1.63	3.2	15.26	2.47	1.96	16
	5	1.64	3.1	15.25	2.54	1.89	17
II	1	1.97	2.3	22.54	5.62	1.17	25
	2	1.97	2.3	22.54	5.62	1.17	25
	3	1.97	2.3	22.54	5.62	1.17	25
	5	1.97	2.3	22.89	6.55	1.17	29
	6	1.97	2.3	22.89	6.55	1.17	29
	7	1.97	2.3	22.89	6.55	1.17	29
	8	1.97	2.1	26.1	10.23	1.07	39
III	1	2.4	3.1	15.19	3.83	1.29	25
	2	2.4	3.1	14.75	3.68	1.29	25
	3	2.4	3.1	15.19	3.83	1.29	25
	4	2.4	3.1	14.75	3.68	1.29	25
IV	2	1.6	2.4	28.01	6.41	1.50	23
	4	1.6	2.4	31.85	8.56	1.50	27
	7	1.6	2.3	27.8	8.24	1.44	30
	9	1.6	2.2	31.85	10.42	1.38	33

displacements predicted by TORSA without and with the consideration of auxiliary measures, respectively. In this paper, the effects of auxiliary measures are equivalent to an increase in undrained shear strength for soft clay, and that in turn leads to an increase in factor of safety against basal heave and a decrease in wall deformation, while the stiffness ratio $EI / \gamma_w h_{avg}^4$ defined by Clough *et al*. (1989) remains unchanged. As shown in Table 10, the F_b values of these four cases magnified by an average factor of 1.93, 1.15, 1.29 and 1.45, respectively. It has to be pointed out that there are differences on the layout of auxiliary measures for each side of a particular site; therefore there are slight variations of the F_b values as shown in Table 10. As for the wall deformation with the consideration of auxiliary measures, δ_{design} drastically reduced to 16%, 29%, 25% and 28% of $\delta_{baseline}$ for these four cases, respectively. Though $EI / \gamma_w h_{avg}^4$ remains the same for these four cases, the effects of auxiliary measures have a positive impact on the overall stiffness of the retaining system, leading to a significant reduction in wall deformation.

With the effects of auxiliary measures being considered, the factors of safety against basal heave (F_b), the maximum wall displacements predicted by TORSA (δ_{design}), the maximum wall displacements measured in the field ($\delta_{in\text{-}situ}$), and the maximum wall displacements predicted by Clough's design curves (δ_{Clough}) are summarized and listed in Table 11. Numbers shown in Table 11 reveal that most of the measured wall displacements are lower than the values predicted by TORSA ($\delta_{in\text{-}situ} < \delta_{design}$), and this phenomenon is much more evident for small or mid-size excavation sites such as Cases I and III. It is speculated that a pronounced 3-dimensional effect or a preloading effect by jet grouting may have helped in limiting the wall displacement to a level much lower than expected.

Also depicted in Table 11, the factors of safety against basal heave for Cases I and III are all greater than 3 ($F_b > 3$), exceeding the applicable range of design curves shown in Fig. 2. Even if the Clough's design curves are extrapolated to F_b higher than 3, the predicted wall displacements for Cases I and III are still much higher than the field data, *i.e.*, $\delta_{Clough} >> \delta_{in\text{-}situ}$. Cases II and IV are considered as large sites, the behavior of excavation can be better regarded as a plane strain condition, therefore it is expected that the field measurements should not be too far away from the Clough's predictions, which is the case shown in Table 11.

Field data of these four cases are plotted on Fig. 11 along with the design curves proposed by Clough *et al*. (1989) for comparison. To better present the field data on Clough's chart, the average F_b and $\delta_{in\text{-}situ} / H_e$ of each case listed in Table 11 were used instead in plotting Fig. 11. The values of average F_b are 3.15, 2.28, 3.1 and 2.32 for Cases I to IV, respectively. And values of average $\delta_{in\text{-}situ} / H_e$ are 0.025%, 0.26%, 0.031% and 0.21% for Cases I to IV, respectively. For large construction sites dominated by plane strain conditions such as Cases II and IV, the observed wall displacements are in good agreement with Clough's design curves as indicated in Fig. 11 and Table 11. As for small construction sites with pronounced 3-dimensional effect such as Cases I and III, the observed wall displacements are well below Clough's design curves. In summary, It appears that Clough's design curves are still applicable as a guide for modern excavation design, provided that the factor of safety against basal heave is less than 3 ($F_b < 3$). However, for excavations with stringent requirements on wall displacements, Clough's design curves may have to be further extended to cover the area with the factor of safety against basal heave higher than 3 ($F_b > 3$).

Table 11 Comparison between design and in-situ displacements

Case	SID	F_{b_design}	δ_{design} (mm)	$\delta_{in\text{-}situ}$ (mm)	$EI / \gamma_w h_{avg}^4$	δ_{design} / H_e (%)	$\delta_{in\text{-}situ} / H_e$ (%)	δ_{Clough} / H_e (%)
I	1	3.2	24.7	1.6	986	0.14	0.01	*
	3	3.1	25.4	3.7	986	0.15	0.02	*
	4	3.2	24.7	3.9	986	0.14	0.02	*
	5	3.1	25.4	7.8	986	0.15	0.05	*
II	1	2.3	56.2	54.1	540	0.28	0.32	0.24
	2	2.3	56.2	36.0	540	0.28	0.21	0.24
	3	2.3	56.2	72.0	540	0.28	0.42	0.24
	5	2.3	65.5	45.2	540	0.33	0.23	0.24
	6	2.3	65.5	18.8	540	0.33	0.09	0.24
	7	2.3	65.5	52.9	540	0.33	0.26	0.24
	8	2.1	102.3**	129.7	540	0.48	0.65	0.25
III	1	3.1	38.3	0.6	829	0.18	0.003	*
	2	3.1	36.8	7.5	829	0.17	0.03	*
	3	3.1	38.3	3.9	829	0.18	0.02	*
	4	3.1	36.8	15.9	829	0.17	0.07	*
IV	2	2.4	64.1	55.8	2122	0.20	0.17	0.18
	4	2.4	85.6	55.4	2122	0.26	0.17	0.18
	7	2.3	82.4	67.9	2122	0.25	0.21	0.19
	9	2.2	104.2	87.2	2122	0.32	0.27	0.19

* : δ_{Clough} out of bound **: Abnormal data

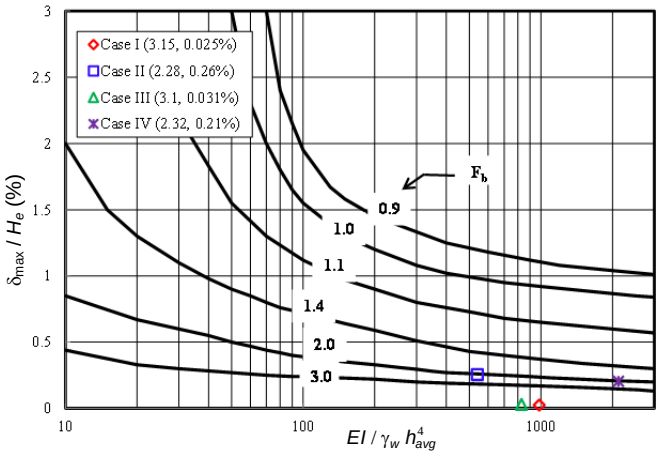

Note: numbers in parenthesis are average F_b and $\delta_{in\text{-}situ} / H_e$ for each case

Fig. 11 Relationship between the average wall displacement and system stiffness for Cases I to IV

7. DISCUSSIONS

If wall deformation is the subject of discussion for a deep excavation project, then the issue of an adequate system stiffness must be carefully addressed. The original system stiffness as defined by Clough *et al*. (1989) did not incorporate the effects of auxiliary measures that are widely used in contemporary deep excavation design to minimize wall displacement, that makes the selection of an appropriate system stiffness difficult in a routine design. This paper establishes an approach that quantifies the effects of soil improvement, buttress wall and cross wall as an increase in soil strength, and that in turn relates the effects of these auxiliary measures to an increase in factor of safety against basal heave. From there, the original design curves developed by Clough *et al*. (1989) can again be used in contemporary excavation design. It is debatable that a single parameter, namely, the factor of safety against basal heave, can fully represent the complex 3-dimensional behavior of a deep excavation, not to mention that the excavation behavior is further complicated by the adoption of auxiliary measures, but at least it reveals the positive effect of these auxiliary measures in limiting wall displacement.

Another issue needs further discussion is the stiffness of bracing system consisted of *H*-section steel struts. In a routine design, the horizontal struts are considered as elastic springs with specified spring constants. The spring constant of bracing system is a function of its section modulus, horizontal spacing of the layout, and width or length of the construction site. These factors are essential for the determination of spring constant as well as the equivalent stiffness of bracing system. However, they are not part of system stiffness equation as defined by Clough *et al*. (1989). The magnitude of preloading also has a significant impact on the wall deformation, but this factor was not included in the original system stiffness either. Only one factor of the bracing system, the average vertical spacing of bracing system, is included in the calculation of system stiffness, which raises the question that the stiffness of bracing system is not well represented. However, the contemporary excavation design adopts a standard bracing layout that has almost the identical spacing, dimension and preload for each level of horizontal strut, and that leaves the vertical spacing as the most influential factor in a bracing design. In other words, how many levels of horizontal strut essentially governs the performance of a standard bracing system. Therefore, using the average vertical spacing as the lone factor to represent the behavior of bracing system turns out to be a reasonable choice.

For top-down excavations that use floor slabs as excavation supports, it is apparent that the section modulus of floor slab per unit width is much higher than that of the *H*-section steel used for bottom-up excavations, leading to the illusion that the floor slabs could provide better resistance to counter lateral movement of retaining wall. Though much lower in section modulus per unit width than reinforced concrete floor slab, the *H*-section steel has the advantage that it can be preloaded to offset the disadvantage of a weaker support. A study (Jeng 1991) comparing the wall deformations of top-down and bottom-up excavations in Taipei area shows that the ratios between maximum wall displacement and excavation depth are almost identical for these two different excavation schemes. In summary, it appears that there is no need to differentiate between top-down and bottom-up schemes in evaluating the system stiffness of excavations.

How factor of safety against basal heave is computed should also be discussed. In its original form, the factor of safety against basal heave includes excavation depth, site width, undrained shear strength of clay above and below dredge line as the parameters. The excavation depth and site width are straight forward numbers for a specific project, however, the undained shear strength of clay used in the calculation cannot be clearly defined. Firstly, the undrained shear strength of clay usually varies with depth, average values for clay above and below dredge line must be carefully assessed beforehand. Secondly, the use of auxiliary measures further complicates the calculation as soil improvement, buttress wall and cross wall improve only the ground within excavation, *i.e.*, the undrained shear strength of clay within the excavation is increased as a result of the auxiliary measures, but the undrained shear strength of clay outside of excavation remains unchanged. To be accurate on the calculation of factor of safety against basal heave, a weighted average undrained shear strength for clay below dredge line has to be considered. Admittedly, this intriguing practice of finding a representative undrained shear strength to calculate the factor of safety against basal heave is difficult for engineers, but by doing so, the factor of safety against basal heave not only relates to the stability of excavation, but also serves as an index reflecting the combined effects soil strength, site dimension, and auxiliary measures.

8. CONCLUSIONS

This paper addresses issues on how wall displacement can be estimated when auxiliary measures such as ground improvement, buttress wall and cross wall are adopted in the excavation design. Basically, the factor of safety against basal heave is re-evaluated to incorporate the effects of auxiliary measures, and this simplified approach allows the designers to utilize Clough's design curves to assess the possible wall deformation. As shown by the case histories, the effective use of ground improvement, buttress wall and cross wall can reduce the wall deformation to less than 0.2% of the excavation depth. However, this very low amount of deformation is sometimes below the applicable range of Clough's design curves, and further studies are required to extend the design curves to displacement zone as low as 0.05% of the excavation depth.

Some excavation cases shown in this paper exhibit observed wall displacements much lower than the predicted ones. The discrepancies between prediction and field performance can be attributed to the under estimation of 3-dimensional site effect or the collateral preloading effect induced by ground improvement. Further studies on these factors unaccounted for in this paper are also required.

This paper also showed that the design curves sketched by Clough *et al*. provide reasonable predictions on wall deformation if the factor of safety against basal heave is less than 3. But even for a good prediction, the magnitude of wall deformation can still reach 0.2% of the excavation depth, exceeding the limits required to protect fragile adjacent buildings. In summary, the requirements on displacement control for contemporary deep excavation design have far exceeded the applicable range of conventional design chart, it is deemed necessary to revise the definition of system stiffness and extend the design curves into very low deformation zone to serve the need for contemporary excavation design.

NOTATIONS

B width of excavation
c cohesion of sandy soil
c_m equivalent cohesion of the improved sandy soil
c' effective cohesion
EI flexural stiffness of retaining wall
F_b factor of safety against basal heave
$F_{b\_baseline}$ factor of safety against basal heave (effect of auxiliary measures not included)
F_{b_design} factor of safety against basal heave (effect of auxiliary measures included)
H_e excavation depth
h_{avg} average vertical spacing of bracing system
I_r improvement ratio
K_h horizontal modulus of subgrade reaction
K_p coefficient of passive resistance
K_h^* equivalent horizontal modulus of subgrade reaction (effect of buttress walls included)
L length of buttress wall
N blow count of standard penetration test
N_B number of buttress walls
q_u unconfined compressive strength of the improvement piles
S system stiffness
s_u undrained shear strength
s_{um} undrained shear strength of the improved ground
s_u^* equivalent undrained shear strength (effect of buttress and cross walls included)
α empirical correction factor for improvement piles
ϕ_m equivalent friction angle of the improved sandy soil
ϕ friction angle of the sandy soil
ϕ' effective friction angle
γ_t total unit weight of soil
γ_w unit weight of water
σ'_v effective overburden pressure
$\delta_{baseline}$ maximum wall displacements predicted by TORSA without the consideration of auxiliary measures
δ_{design} maximum wall displacements predicted by TORSA with the consideration of auxiliary measures
$\delta_{in\text{-}situ}$ measured in-situ maximum wall displacements
δ_{Clough} maximum wall displacements predicted by Clough's design curves
δ_{hm} maximum wall displacement

REFERENCES

Chien, M.C., Shih, C., and Hsieh, H.S. (2004). "On the design and construction practice of deep excavation." *Sino-Geotechnics*, **100**, 135–152 (in Chinese).

Clough, G.W., Smith, E.M., and Sweeney, B.P. (1989). "Movement control of excavation support systems by iterative design." *Proceedings, ASCE Foundation Engineering: Current Principles and Practices*, **2**, 869–884.

Clough, G.W. and O'Rourke, T.D. (1990). "Construction induced movements of in situ walls." *Design and Performance of Earth Retaining Structures, ASCE Special Publication*, **25**, 439–470.

Finno, R.J., Blackburn, J.T., and Roboski, J.F. (2007). "Three-dimensional effects for supported excavations in clay." *Journal of Geotechnical and Geoenvironmental Engineering*, ASCE, **133**(1), 30–36.

Hsieh, H.S., Chien, M.C., and Chen, C.T. (1991). "Design, construction and performance of a deep excavation in soft clay." *Proceedings, First Young Asian Geotechnical Engineers Conference*, Asian Institute of Technology, Bangkok, 41–50.

Hsieh, P.G. and Ou, C.Y. (1998). "Shape of ground surface settlement profiles caused by excavation." *Canadian Geotechnical Journal*, **35**(6), 1004–1017.

Hsieh, H.S. and Lu, F.C. (1999). "A note on the analysis and design of diaphragm wall with buttresses." *Sino-Geotechnics*, **76**, 39–50 (in Chinese).

Hsieh, H.S., Wang, K.R., and Yang, Y.C. (2002). "Outward deformation of diaphragm wall induced by jet grouting." *Sino-Geotechnics*, **93**, 33–42 (in Chinese).

Hsieh, H.S., Wang, C.C., and Ou, C.Y. (2003). "Use of jet grouting to limit diaphragm wall displacement of a deep excavation." *Journal of Geotechnical and Geoenvironmental Engineering*, ASCE, **129**(2), 146–157.

Hsieh, H.S., Hsu, W.T., and Chou, C.J. (2015). "Incorporating 3-dimensional effect in the design of a small excavation in soft clay." *Proceedings, International Conference on Soft Ground Engineering*, Singapore, 669–677.

Jeng, S.H. (1991). *Numerical Analyses for Deep Excavations in Taipei Area*, Master Thesis, Department of Construction Engineering, National Taiwan Institute of Technology (in Chinese).

Kuo, C.J., Lin, Y.K., Hung, C.L., Hsia, P.Y., Chang, W.H., Shih, C.S., and Lin, Y.C. (2014). "Case study of urban renewal excavation utilizing original diaphragm wall." *Sino-Geotechnics*, **140**, 49–56 (in Chinese).

Ou, C.Y., Chiou, D.C., and Wu, T.S. (1996). "Three-dimensional finite element analysis of deep excavations." *Journal of Geotechnical Engineering*, ASCE, **122**(5), 337–345.

Ou, C.Y., Lin, Y. L., and Hsieh, P.G. (2006). "Case record of an excavation with buttress walls and cross walls." *Journal of GeoEngineering*, **1**(2), 79–86.

Ou, C.Y. (2006). *Deep Excavation; Theory and Practice*, Taylor and Francis, Netherland.

Terzaghi, K. (1967). *Theoretical Soil Mechanics*, John Wiley & Sons, New York.

TORSA (2016). *Taiwan Originated Retaining Structure Analysis*, Sino-Geotechnics Research and Development Foundation (computer code).

Tsai, J.S. (1994). "A post-study on the stability analysis of an excavation within soft ground." *Sino-Geotechnics*, **45**, 13–22 (in Chinese).

Woo, S.M. (1992). "Methods of building protection, design and construction." *Sino-Geotechnics*, **40**, 51–61 (in Chinese).

Woo, S.M. and Moh, Z.C. (1990). "Geotechnical characteristics of soils in the Taipei basin." *Special Taiwan Session, Tenth Southeast Asian Geotechnical Conference*, Taipei.

Wu, C.H. (1989). *Effect of Grouting on the Behavior of Deep Excavation*, Master Thesis, Department of Construction Engineering, National Taiwan Institute of Technology (in Chinese).